

## Supplementary Materials for

### **3D hESC exosomes enriched with miR-6766-3p ameliorates liver fibrosis by attenuating activated stellate cells through targeting the TGF $\beta$ RII-SMADS pathway**

Ning Wang<sup>1,2‡</sup>, Xiajing Li<sup>2,3‡</sup>, Zhiyong Zhong<sup>1,2‡</sup>, Yaqi Qiu<sup>2‡</sup>, Shoupei Liu<sup>2</sup>, Haibin Wu<sup>2</sup>, Xianglian Tang<sup>1,2</sup>, Chuxin Chen<sup>4</sup>, Yingjie Fu<sup>2</sup>, Qicong Chen<sup>1,2</sup>, Tingting Guo<sup>2</sup>, Jinsong Li<sup>5,6</sup>, Shuai Zhang<sup>7</sup>, Mark A Zern<sup>8</sup>, Keqing Ma<sup>9</sup>, Bailin Wang<sup>10</sup>, Yimeng Ou<sup>11</sup>, Weili Gu<sup>7\*</sup>, Jie Cao<sup>12\*</sup>, Honglin Chen<sup>2,13,14,15,16\*</sup>, Yuyou Duan<sup>2,13,14,15,16\*</sup>

1. School of Biomedical Sciences and Engineering, Guangzhou International Campus, South China University of Technology, Guangzhou 510006, P.R. China.

2. Institutes for Life Sciences and School of Medicine, South China University of Technology, Guangzhou 510006, P.R. China.

3. School of Medicine, South China University of Technology, Guangzhou 510180, P. R. China.

4. School of Biology and Biological Engineering, South China University of Technology, Guangzhou 510006, P.R. China.

5. State Key Laboratory of Cell Biology, Shanghai Key Laboratory of Molecular Andrology, Shanghai Institute of Biochemistry and Cell Biology, Center for Excellence in Molecular Cell Science, Chinese Academy of Sciences, Shanghai 200031, China.

6. University of Chinese Academy of Sciences, Shanghai 200031, China.

7. Department of Gastroenterology and Hepatology, Guangzhou Digestive Disease Center, Guangzhou First People's Hospital, School of Medicine, South China University of Technology, Guangzhou 510180, P. R. China.

8. Department of Internal Medicine, University of California Davis Medical Center, Sacramento, California 95817, USA.

9. Department of Hepatobiliary pancreatic surgery, Huadu District People's Hospital of Guangzhou, Guangzhou, 510800, P. R. China.

10. Department of General Surgery, Guangzhou Red Cross Hospital, Jinan University, Guangzhou, 510220, P. R. China.

11. Department of general surgery, the First Affiliated Hospital of Guangdong Pharmaceutical University, Guangzhou 510080, P. R. China.

12. Department of general surgery, Guangzhou Digestive Disease Center, Guangzhou First People's Hospital, School of Medicine, South China University of Technology, Guangzhou 510180, P. R. China.

13. National Engineering Research Center for Tissue Restoration and Reconstruction, South China University of Technology, Guangzhou 510006, P. R. China.

14. Key Laboratory of Biomedical Engineering of Guangdong Province, South China University of Technology, Guangzhou 510006, P. R. China.

15. Key Laboratory of Biomedical Materials and Engineering of the Ministry of Education, South China University of Technology, Guangzhou 510006, P. R. China.

16. Innovation Center for Tissue Restoration and Reconstruction, South China University of Technology, Guangzhou 510006, P. R. China.

‡ Ning Wang, Xiajing Li, Zhiyong Zhong and Yaqi Qiu contributed equally to this work.

**\* Correspondence to:**

Yuyou Duan, Ph.D.

Laboratory of Stem Cells and Translational Medicine

Institutes for Life Sciences

School of Medicine

South China University of Technology

No.382 Waihuan East Road, Suite 406

Higher Education Mega Center

Guangzhou 510006, P.R.China

Telephone: +86 20 3939 0970

E-mail: yuyouduan@scut.edu.cn

Honglin Chen, Ph.D.

Laboratory of Stem Cells and Translational Medicine

Institutes for Life Sciences

School of Medicine

South China University of Technology

382 Waihuan East Road, Suite 406

Higher Education Mega Center

Guangzhou 510006, P.R.China

Telephone: +86 20 3939 0970

E-mail: chenhl@scut.edu.cn

Jie Cao, M.D., Ph.D.

Department of general surgery

Guangzhou Digestive Disease Center

Guangzhou First People's Hospital

School of Medicine

South China University of Technology

No.1 Panfu Road

Guangzhou 510180, P. R. China

Telephone: +86 20 8104 8181

E-mail: eycaojie@scut.edu.cn

Weili Gu, M.D., Ph.D.

Department of Gastroenterology and Hepatology

Guangzhou Digestive Disease Center

Guangzhou First People's Hospital

School of Medicine

South China University of Technology

No.1 Panfu Road

Guangzhou 510180, P. R. China

Telephone: +86 20 8104 8281

E-mail: lili-6423@163.com

**This file includes:**

Materials and Methods

Figures S1 to S15

Tables S1 to S4

## **Methods**

### **hESC Culturing**

The hESC line was cultured in 2D and 3D conditions respectively, briefly, hESCs dissected from culture condition with feeder cells [44] were moved to the Matrigel-coated plate for 2D culture and the ultra-low attachment plate (Corning) for 3D culture, and cultured with serum-free mTesR1 medium (STEMCELL).

### **Exosome Isolation**

2D-Exo and 3D-Exo were isolated as previously described [20]. Supernatants were collected from hESC culture in mTesR1 medium without FBS and subsequently subjected to sequential centrifugation steps at 500 g for 10 minutes to remove cells, at 2000 g for 20 minutes to remove apoptotic bodies, and at 5000 g for 30 minutes to remove cell debris. The resulting supernatant was then filtered using 0.22  $\mu\text{m}$  filters (Millipore, Merck, Germany), and hESC-Exosomes were harvested by centrifugation at 130000 g for 2 hours in a SW32 Ti rotor (Beckman Coulter, L-100XP Ultracentrifuge, CA). The pellet was resuspended in PBS and subsequently ultracentrifuged at 130000 g for another 2 hours to remove the contaminating proteins.

### **Transmission Electron Microscope (TEM)**

TEM (Talos F200C, Thermo Fisher, MA) was performed at 200 kV to visualize and examine the morphology of hESC-Exosomes. Samples were deposited on copper grids covered with a carbon support film (Zhongjingkeyi Technology, Beijing, China) and dried for 2 minutes at room temperature. The excess fluid was removed with a piece of

filter, and the samples were negatively stained with 2% uranyl acetate for 30 seconds.

Finally, these samples were air-dried for 60 minutes, and images were captured.

### **Nanoparticle Tracking Analysis**

The size, concentration, and zeta potential of hESC-Exosomes were determined using NTA (Particle Metrix, Germany). The parameters of the measurement were set using 100 nm polystyrene-latex beads as standards. hESC-Exosomes were prepared by the dilutions at 4000- and 2000-folds using distilled deionized water respectively, to achieve the objects at the number between 20 and 100 per frame. Each sample was measured in triplicate at the camera setting with an acquisition time of 60 seconds.

### **Western Blot**

The protein concentrations were determined using a bicinchoninic acid (BCA) protein assay reagent (Pierce, Rockford, IL) according to the manufacturer's instructions. hESC-exosomes or the cells were lysed with ice-cold lysis buffer (150 mM NaCl, 50 mM Tris-Cl (pH 7.5), 1 mM EDTA, 1% NP-40, 0.1% SDS, 0.25% sodium deoxycholate, 1 mM PMSF, 1 mM  $\beta$ -glycerophosphate, 1 mM NaF, 1 mM Na<sub>3</sub>VO<sub>4</sub>, and protease inhibitor cocktail tablets (Roche Molecular BioChemicals, Indianapolis, IN). Aliquots containing 30  $\mu$ g of protein were mixed with loading buffer, followed by denaturation at 95 °C for 5 minutes. Proteins were separated by 12% sodium dodecyl sulfate polyacrylamide gel electrophoresis (SDS-PAGE; Invitrogen, Carlsbad, CA) and transferred to polyvinylidene difluoride membranes (PVDF) (Millipore, Watford, UK). The membranes were blocked with 5% non-fat milk in tri-sec-buffered saline/ Tween-

20 (TBST) buffer (20 mM Tris-HCl, pH 7.6, 136 mM NaCl and 0.1% Tween-20), and then probed overnight with primary antibodies, then the membranes were incubated with horseradish peroxidase-conjugated secondary antibodies for 2 hours at room temperature. Protein signals were visualized using the West Pico Chemiluminescent Substrate Kit (Pierce, Rockford, IL). The primary and secondary antibodies were listed in Supplemental Table S4.

### **hESC-Exosome Labeling**

Purified 2D-Exo and 3D-Exo were labeled with PKH26 Red Fluorescent Cell Linker Kit according to the manufacturer's protocol. The extracted hESC-exosomes and lipophilic red fluorescent dye PKH26 (4  $\mu$ M) (Sigma, MIDI26) were fully mixed and incubated at 37 °C for 30 minutes. After incubation, the mixture was sucked into a 100 KDa MWCO ultra-filtration centrifuge tube, 10 times the volume of PBS, was gently blown and mixed, centrifuged at 4 °C for 30 minutes, the unbound PKH26 dye was removed, the concentrated liquid in the ultra-filtration centrifuge tube was collected, and the bacteria were removed by a 0.22  $\mu$ m filter. The filtered concentrated liquid was moved into the new EP tube and preserved at 4 °C.

### **Activation of LX2 Cells and Treatment with hESC-Exosomes**

In the logarithmic proliferation phase of LX2 cells, the cells were digested and subcultured by trypsin.  $1.25 \times 10^5$  cells per well were seeded in the six-well plate, and the microslide treated with polylysine were placed in the dish pool. When LX2 cells were adherent to the wall (> 6 hours), TGF- $\beta$ 1 (TGF $\beta$ , Peprotech, 100-21-50) was

added to induce activation of LX2 cells at the final concentration of 10ng/mL for 48 hours. 20 µg of 2D-Exo and 3D-Exo labeled with PKH26 (4 µM;  $\lambda_{\text{ex}} = 565 \text{ nm}$ ,  $\lambda_{\text{em}} = 594 \text{ nm}$ ) were respectively added. The same volume of PBS was added to the control group. The cells were examined 24 hours after treatment.

### **Observation of Intracellular Localization of Exosomes in Cells by Laser Scanning Microscopy (LSM)**

LX2 cells were cultured in 6-well plates with the cell number at  $1 \times 10^5$  cells per well and adhered overnight. PKH26-labeled 2D-Exo and 3D-Exo were respectively added into LX2 cells and incubated at 37 °C in dark for 24 hours, discarded culture medium, and washed with PBS for 3 times. Afterward, the cells were fixed using 4% paraformaldehyde (PFA) (Sangon Biotech, Shanghai, China) for 10 minutes, and then washed with PBS three times. The fixed cells were incubated with primary antibody against  $\alpha$ -Tubulin (CST, 3873s) overnight at 4 °C, and then incubated with Alexa Fluor 488-conjugated goat anti-rabbit IgG (CST, 4412s). The cell nuclei were counterstained with 4, 6-diamidino-2-phenylindole (DAPI) for 10 minutes and imaged using LSM (Ni-E-A1, Japan).

### **Determination of Intracellular Calcium Concentration**

Differently treated-LX2 cells were washed three times with PBS, and incubated with Fluo-3 AM (Beyotime, S1056) at 5 mM at 20-37 °C for 10-60 minutes, then washed for 3 times with PBS. Fluo-3 fluorescence was detected by flow cytometry to determine the changes in intracellular calcium concentration.

### **Terminal Deoxynucleotidyl Transferase-Mediated dUTP Eick-End Labeling (TUNEL) assay**

A TUNEL assay was performed to evaluate the apoptotic cells of liver tissues. The tissues were fixed with 4% PFA and post-fixed in a pre-chilled solution containing ethanol and acetic acid mixed at 2:1 for 5 minutes at  $-20^{\circ}\text{C}$ . After fixation, samples were processed according to the manufacturer's instructions (Beyotime, C1086) and imaged using LSM (Ni-E-A1, Japan). Quantitative analysis was accomplished using ImageJ software (National Institutes of Health, USA).

### **Wound Healing Assay**

$5 \times 10^5$  LX2 cells were seeded in the six-well plate, when the cells were adherent ( $> 6$  hours),  $\text{TGF}\beta$  was added to induce activation of LX2 cells at the final concentration of 10 ng per mL for 48 hours, 20  $\mu\text{g}$  of 2D-Exo and 3D-Exo were respectively added and incubated with LX2 cells. After culturing for 24 hours, the LX2 cells were scratched with a pipette tip, and the cells were then washed three times with PBS to remove the scraped cells, finally, serum-free medium was added for culturing with 5%  $\text{CO}_2$  at  $37^{\circ}\text{C}$ . The scratched areas were imaged and measured using NIH Image J at 0 hour and 24 hours ( $n = 3$ )

### **CFSE assay**

LX2 cell proliferation rate in four different groups were also determined using flow cytometric analysis with a CellTrace CFSE Cell Proliferation Kit ( $1 \times 10^6$  cells/ml in  $5\mu\text{M}$  of CFSE, 0.1% BSA in PBS for 10 minutes, Biolengend). The reaction was

terminated by the addition of 10 volumes of cold RPMI 1640 with 10% FBS. Finally, the CFSE fluorescent staining was analyzed by flow cytometry. CFSE assays were performed in triplicate. When cells undertook divisions, the CFSE was distributed to daughter cells equally and CFSE fluorescence decreased in daughter cells. Briefly, the progressive loss of CFSE fluorescence is a hallmark of the cell proliferation.

### **Cell Viability Assay**

Briefly, LX2 cells in the above groups were seeded at 5,000 cells per well in a 96-well plate and allowed to settle overnight. Cell proliferation of LX2 cells was measured using a Cell Counting Kit-8 (Beyotime, C0037). CCK-8 reagent was added to each well and incubated for 1, 2, 4 and 6 hours respectively. Absorbance was read at 450 nm and recorded using a microplate spectrophotometer.

### **Teratoma Formation Assay**

2D-hESCs, 3D-hESCs and their respective hESC-Exosomes were collected, and approximately  $1 \times 10^6$  cells of hESCs and 100 ug of hESC-Exosomes were subcutaneously injected into immunodeficient NDG mice (around 5 weeks old) (Biocytogen Co., Ltd, Beijing, China). 6 NDG mice were treated in each group. Teratomas generally developed within 6-8 weeks, and the animals were sacrificed before the tumor sizes exceeded 1.5 cm in diameter. The teratomas were then embedded in paraffin and processed for hematoxylin and eosin (HE) staining.

### **Immunofluorescence Staining**

The cells were fixed in 4% PFA at room temperature for 15 minutes and blocked with blocking buffer that contained 0.2% Triton X-100 (Sigma-Aldrich, T8787) and 3% normal goat serum (Jackson Immuno Research, 017-000-121) in PBS at room temperature for 45 minutes, then the cells were incubated with primary antibodies at 4 °C overnight. Next day, primary antibodies were replaced with secondary antibodies conjugated with fluorescences (CST, 7074s and 7076s) after washing with PBS, and the cells with antibodies were incubated at room temperature for 1 hour. The nuclei were stained with DAPI. The primary and secondary antibodies were listed in Supplemental Table S4.

### **Flow cytometric Analysis**

Single cell suspensions from 2D-hESCs and 3D-hESCs culturing were prepared using GCDR (STEMCELL, 07174), washed in PBS, then resuspended in 0.1% BSA in PBS. Anti-TRA-1-81-PE and anti-SSEA4-PE (STEMCELL Technologies) and PE Mouse IgG1  $\kappa$  Isotype Control (BD) were added to cell suspensions to incubate at 4 °C for 30 minutes in the dark. Intracellular staining for OCT4 were performed according to the manufacturer's instructions (STEMCELL Technologies). Cells were examined by flow cytometry. Data were analyzed using Flowjo software (Flowjo, Ashland, USA).

### **Detection of Serological Markers and Liver Injury in Fibrotic Mice**

4 weeks after intravenously receiving CCL<sub>4</sub> and 56% alcohol gavage, the mice fasted 12 hours before they were sacrificed. Serum was collected by centrifugation of eyeball blood for testing Aspartate Transaminase (AST) (Solarbio, BC1560), Alanine

transaminase (ALT) (solarbio, BC1550), albumin (ALB) (Ek-Bioscience, Ek-M20152) and Total bilirubin (TBIL) (GTX, YS01266B) using an automatic biochemical analyzer. Liver tissue samples were retained separately, and fixed in 4% PFA for histopathological analysis. In addition, the remaining liver tissues were first placed in liquid nitrogen for quick cryopreservation and then transferred into -80 °C for storage.

### **Two-photon excited fluorescence (TPEF) imaging of PKH26-labeled hESC-Exosomes Distributed in Various Organs of Mice in vivo and ex vivo**

The hepatic fibrosis model mice were injected intravenously with 100 µg of PKH26-labeled 2D-Exo and 3D-Exo as well as equal volume PBS (control group). The mice anesthetized at different time points, and tissue samples from mice were imaged to collect fluorescence in stack scan mode by TPEF (Ni-E-A1RMP) with a laser at wavelengths of 1080 nm for PKH26 imaging. During the imaging process, each sample were scanned continuously (a frame of a 2D image) for PKH26 simultaneously at a speed of 10 second per frame. The exposure time of the samples was limited within 30 minutes. The intensities of the signals were analyzed using Image J software.

### **RNA Extraction and Quantitative Polymerase Chain Reaction (qPCR)**

Total RNA was extracted from cells and tissues using RNAiso Plus (Takara, 9109) according to the manufacturer's manuals, MiRNAs of 2D-Exo and 3D-Exo were isolated using the SeraMir Exosome RNA Purification Column Kit (EZBioscience, EZB-exo-RN1). For mRNA detection, complementary DNA (cDNA) was synthesized

from 500 ng of total RNA using a PrimeScript™ RT Master Mix (Takara); for miRNA expression analysis, 500 ng total RNA was reverse-transcribed into cDNA using Mir-X™ miRNA First Strand and Synthesis kit (Takara) as described by the manufacturer's protocol. All qPCR experiments were performed on a real-time PCR machine (ABI, ABI7500) with the QuantiTect SYBR Green PCR Kit (Takara) and specific primers of the genes of interest, and amplification efficiencies were checked by standard curves. Gene expression was quantified by the comparative cycle threshold (Ct) method. The relative amounts of target gene expression were determined by subtracting the Ct values of these genes from the Ct value of the housekeeping gene GAPDH and the abundance of U6 which was used as an internal control for comparison of relative changes in miRNA among different groups ( $\Delta\text{Ct}$ ). The data were presented as  $2^{-(\Delta\Delta\text{CT})}$ . The primer sequences used in this study were listed in Supplemental Table S1.

### **Histology, Immunohistochemistry (IHC) and Immunofluorescence (IF) Assays**

On day 7, 14, 21 and 28 after administration of PBS, 2D-Exo and 3D-Exo, all mice were sacrificed, and the livers were isolated. Liver tissues were immediately fixed in 4% PFA overnight. Afterward, these tissues were embedded in paraffin and sectioned with a thickness of 5  $\mu\text{m}$ , followed HE or Masson's trichrome staining, or ICH assay. The slices obtained were examined with an optical microscope (Nikon, Japan). Furthermore, another fraction of liver tissue was embedded into OCT compound (Sakura Finetek, Japan) and cut into micron-thick frozen sections with the thickness at 10  $\mu\text{m}$  for IF staining. In brief, the sections for ICH and IF staining were incubated with

primary antibodies, and then incubated with secondary antibodies. Cell nuclei in IF staining were counterstained with DAPI. Image J software was used to binarize the immunofluorescence images taken as previously described.<sup>25</sup> The numbers of positive cells were counted by blinded investigators in 6 randomly selected areas. The primary and secondary antibodies were listed in Supplemental Table S4.

### **miRNA Microarray and Data Analysis**

Agilent Feature Extraction software (version 11.0.1.1) was used to analyze acquired array images. Quantile normalization and subsequent data processing were performed using the GeneSpring GX v14.9 software package (Agilent Technologies). After quantile normalization of the raw data, miRNAs that at least 3 out of 6 samples have flags in Detected (“All Targets Value”) were chosen for further data analysis. Differentially expressed miRNAs with statistical significance between the two groups were identified through Volcano Plot filtering. Differentially expressed miRNAs between the two samples were identified through Fold Change filtering. Hierarchical Clustering was performed using the R scripts. Fold change  $\geq 2.0$  or  $\leq 0.5$  and  $P < 0.05$  were the threshold to filtrate differentially expressed miRNAs. The primer sequences used in this study were listed in Supplemental Table S2 and S3.

### **Target Prediction**

Microarray analysis of miRNAs from 2D-Exo and 3D-Exo, including sample labeling, array hybridization, data collection, and normalization, was performed by Kang Cheng Bio-tech (Shanghai, China) according to the Agilent miRNA Microarray System with

miRNA Complete Labeling and Hyb Kit protocol (Agilent Technology). miRDB V5.0, miRNAMap and TargetScan 7.2 software were used to predict target genes of candidate miRNAs.

### **Dual Luciferase Reporter Assay**

For identifying the binding site between miR-6766-3p and its target TGF $\beta$ RII, the 3' untranslated regions (UTRs) of TGF $\beta$ RII including wild-type (wt) or mutant type (mut) were respectively cloned downstream of the Renilla luciferase (Rluc) gene as fusion gene driven by SV40 promoter in pSI-check2 dual luciferase reporter vector in which the firefly luciferase (fluc) gene is driven by HSV TK promoter (<http://www.hanbio.net>, GenePharma Co., China), and 293T cells as the recipient cells were used for luciferase activity assays. Briefly, cells were first transfected with the recombinant pSI-check2 vector containing the wt or mut TGF $\beta$ RII 3' UTR, then the cells were co-transfected with miR-6766-3p mimics and miR-6766-3p mimics negative control. The protein translation of Rluc from transcribed mRNA of fusion gene depends on the binding between miR-6766-3p and its target site, and the fluc is normally expressed and used as the calibrator. The relative activity Rluc/fluc reflects the expression change of Rluc by miR-6766-3p mimics. The luciferase activities were detected using the Dual-Luciferase Reporter Assay System (Promega, U.S.A.) according to the manufacturer's protocol.

### **Validation of Target miRNA**

$2 \times 10^5$  LX2 cells were added into each well of 24 well plate (>6 hours), primed with TGF $\beta$  for 48 hours and then transfected with miR-6766-3p mimics (50 nM), inhibitors, negative control mimics and negative control inhibitors (100 nM) (Ribobio, Guangzhou) using ribo FECT CP Transfection Kit (Ribobio, Guangzhou) as per manufacturer's instructions for 24 hours. LX2 cells from each group were collected for subsequent analysis.

**Reference:**

20. Hou, D. R. et al. Derivation of Porcine Embryonic Stem-Like Cells from In Vitro-Produced Blastocyst-Stage Embryos. *Sci Rep-Uk* 6 (2016).
44. Zhong, C. Q. et al. Generation of human haploid embryonic stem cells from parthenogenetic embryos obtained by microsurgical removal of male pronucleus. *Cell Res* 26, 743-746 (2016).

**Figure. S1**

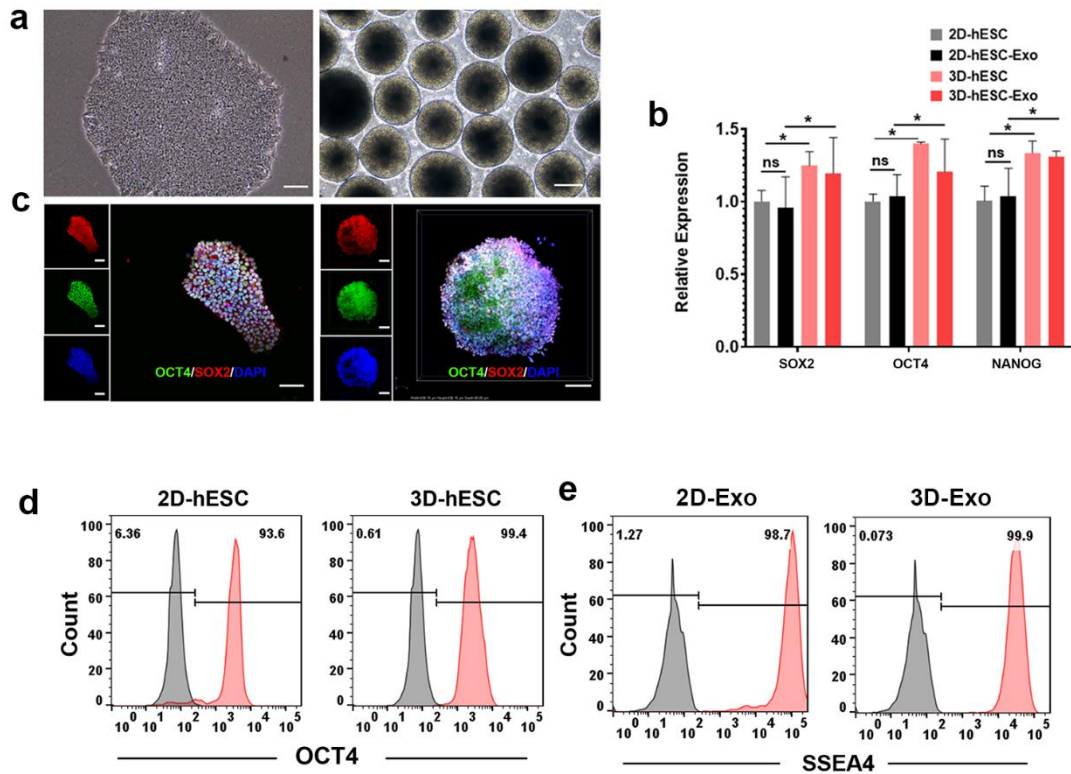


**Figure S1. Characterization of pluripotent markers of cultured hESCs.**

(a) Morphology of hESCs cultured as monolayer (2D) under feeder cell-free condition (left) and in suspension (3D) to form spheroids (right) (scale bar: 100 $\mu$ m) (b) Real-time qPCR analysis of the expression levels of stemness-related genes in 2D and 3D cultured hESCs, respectively. (c) Immunostaining analysis of OCT4 (green) and SOX2 (red) expression in 2D and 3D cultured hESCs using confocal microscopy. DAPI (blue) was used to localize the nuclei of the cells (scale bar: 40 $\mu$ m). The percentage of OCT4<sup>+</sup> cells in hESCs (d) and SSEA4<sup>+</sup> cells hESC-Exosomes (e) was measured by flow cytometry. n=3, Data represent the mean  $\pm$  SEM. \* $P < 0.05$ , \*\* $P < 0.01$ , and \*\*\* $P < 0.001$ .

**Figure. S2**

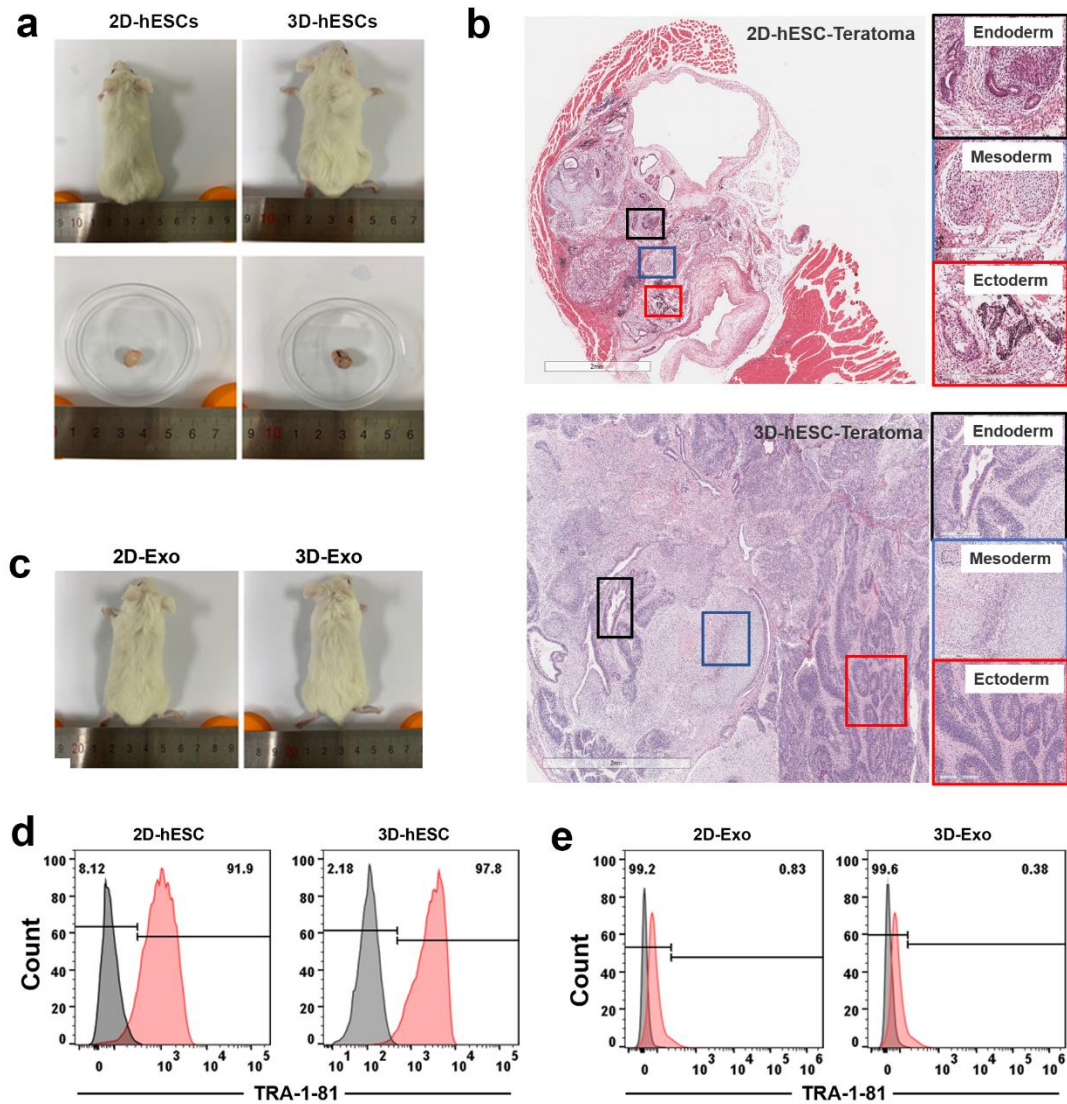


**Figure S2. Evaluation of the capacity of hESCs and hESC-exosomes to form teratomas.**

(a) Teratomas were formed at day 50 post transplantation of hESCs. (b) H&E staining of teratomas from (a). Three germ layers, mesoderm (immature cartilage), endoderm (digestive glands), and ectoderm (epithelium), were found in teratoma tissues. Original magnification, 10 $\times$ , Scale bar, 900 $\mu$ m. (c) No teratoma was formed in mice injected

with hESCs-Exosomes. (d-e) The percentage of TRA-1-81<sup>+</sup> cells in hESCs (d) and hESC-Exosomes (e) was measured by flow cytometry.

Figure. S3

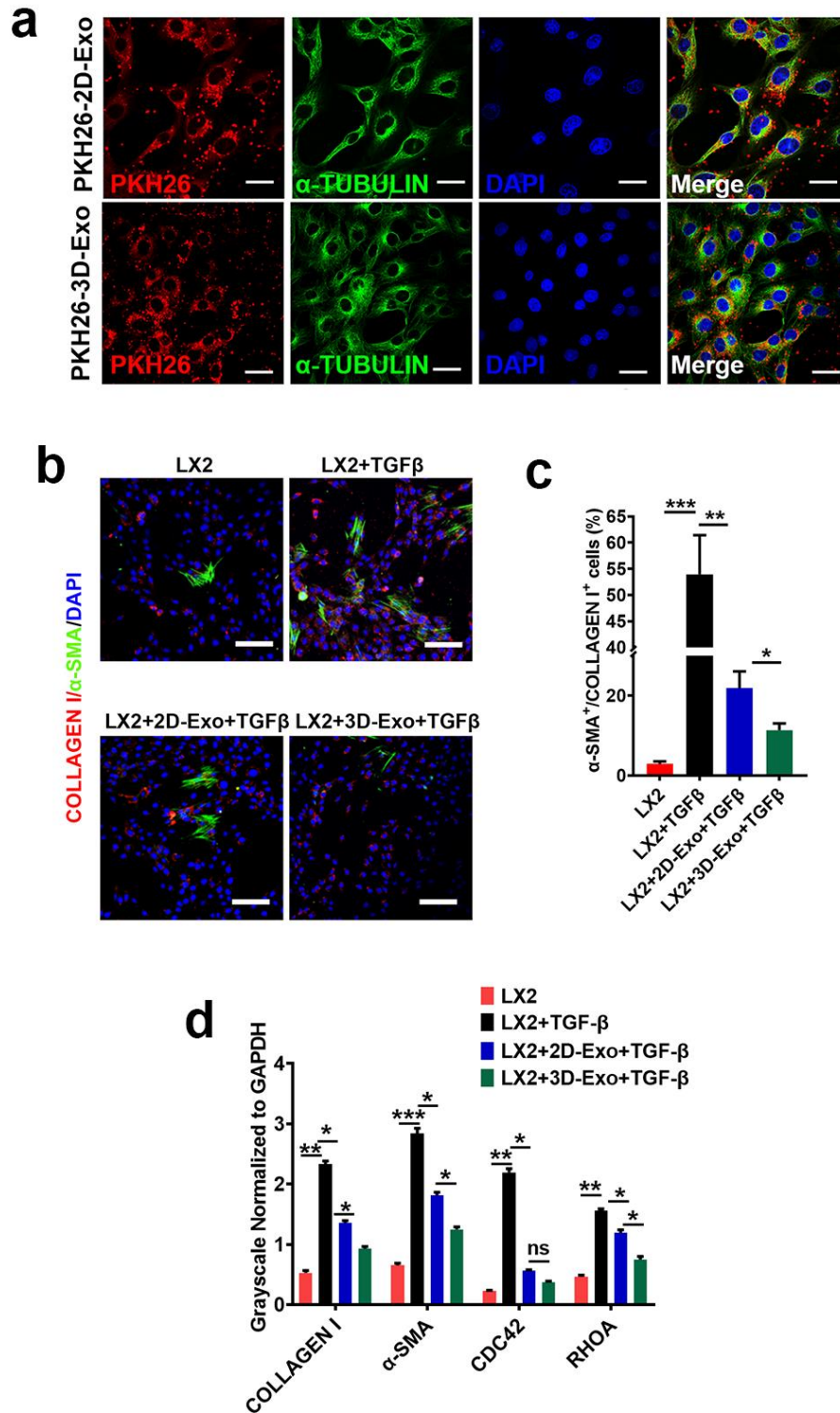
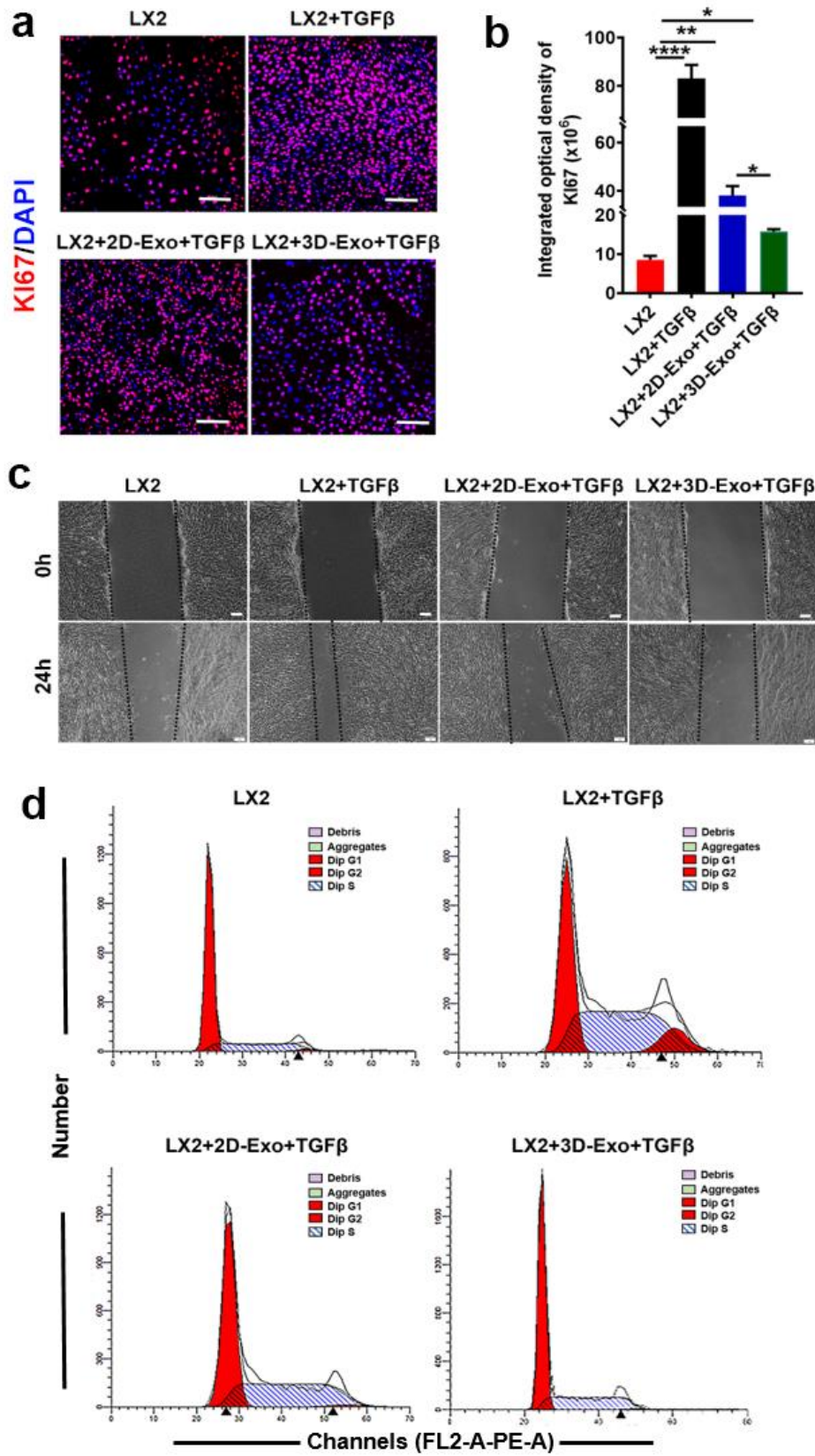


Figure S3. hESC-exosomes internalized by LX2 cells reduced LX2 cells profibrogenic phenotype.

(a) CLSM images of Tubulin immunostaining of internalized PKH26-2D-Exo and PKH26-3D-Exo in LX2 cells. Red: PKH26-2D-Exo and PKH26-3D-Exo. Green: Tubulin. Blue: DAPI. Scale bars, 40 $\mu$ m. (b) CLSM images of immunostaining for  $\alpha$ -SMA and COLLAGEN I in LX2 cells and TGF $\beta$ -induced LX2 cells after treatment with 2D-Exo and 3D-Exo. The colours of Green, red and blue represent the staining for COLLAGEN I,  $\alpha$ -SMA and nuclei. (Original magnification, 20 $\times$ . Scale bar, 40 $\mu$ m). (c) Quantification of the percentage of  $\alpha$ -SMA<sup>+</sup> and COLLAGEN I<sup>+</sup> cells in (b). (d) According to Western blot analysis shown in Fig. 2d, corresponding densitometry of markers COLLAGEN I, CDC42,  $\alpha$ -SMA and RHOA were analyzed in LX2 cells primed with TGF $\beta$  and exposed to 2D-Exo and 3D-Exo for 24 hours. GAPDH was used as a loading control. n=3, Data represent the mean  $\pm$  SEM. \* $P$  < 0.05, \*\* $P$  < 0.01, and \*\*\* $P$  < 0.001.

Figure. S4



**Figure S4. hESC-exosomes modulated proliferation and profibrogenic phenotype of LX2 cells.**

(a) Immunostaining of KI67 in LX2 cells and activated LX2 cells with the treatment of 2D-Exo and 3D-Exo. The colours of Red and blue represent the staining for KI67 and nuclei. Scale bar, 100 $\mu$ m. (b) Quantification of integrated optical density of KI67 in LX2 cells primed with TGF $\beta$  and exposed to 2D-Exo, 3D-Exo or Exo-free supernatant for 24 hours. (c) Wound recovery rates of LX2 cells and activated LX2 with different treatments, modeled by cell scratch assays (Original magnification, 4 $\times$ , Scale bar, 100 $\mu$ m). (d) Cell cycle analysis was used to determine the changes of cell cycle, and results showed that the growth of activated LX2 cells exposed to 2D-Exo or 3D-Exo was significantly inhibited, compared with the TGF $\beta$ -induced group. n=3, Data represent the mean  $\pm$ SEM. \* $P < 0.05$ , \*\* $P < 0.01$ , and \*\*\* $P < 0.001$ .

**Figure. S5**

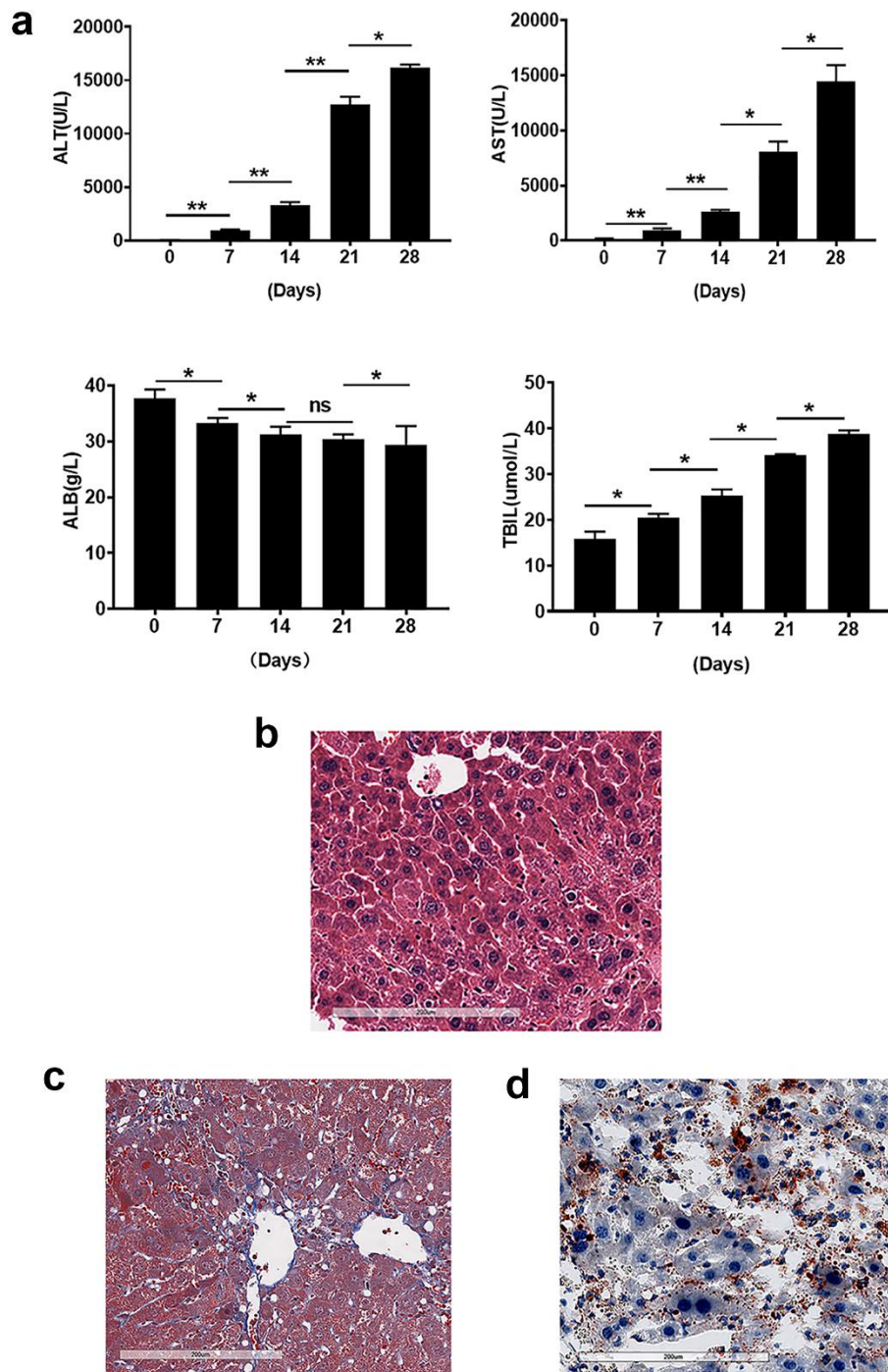


**Figure S5. Evaluation of liver fibrosis induced by CCl<sub>4</sub> and alcohol in mice.**

(a) Serological analysis of AST, ALT, TBIL and ALB in the serum of mice with induced-liver fibrosis. Employing CCl<sub>4</sub> in conjunction with using alcohol had great

effect on decreasing the serum levels of ALB and increasing the serum levels of AST, ALT and TBIL. (b) Representative H&E staining of livers of the fibrosis mice. (c) Collagen deposition in the livers of the fibrosis mice detected by Masson staining. (d) The accumulation of the lipid in the livers of the fibrosis mice detected by Oil Red staining. n=3, Data represent the mean  $\pm$ SEM. \* $P < 0.05$ , \*\* $P < 0.01$ , and \*\*\* $P < 0.001$ .

Figure. S6

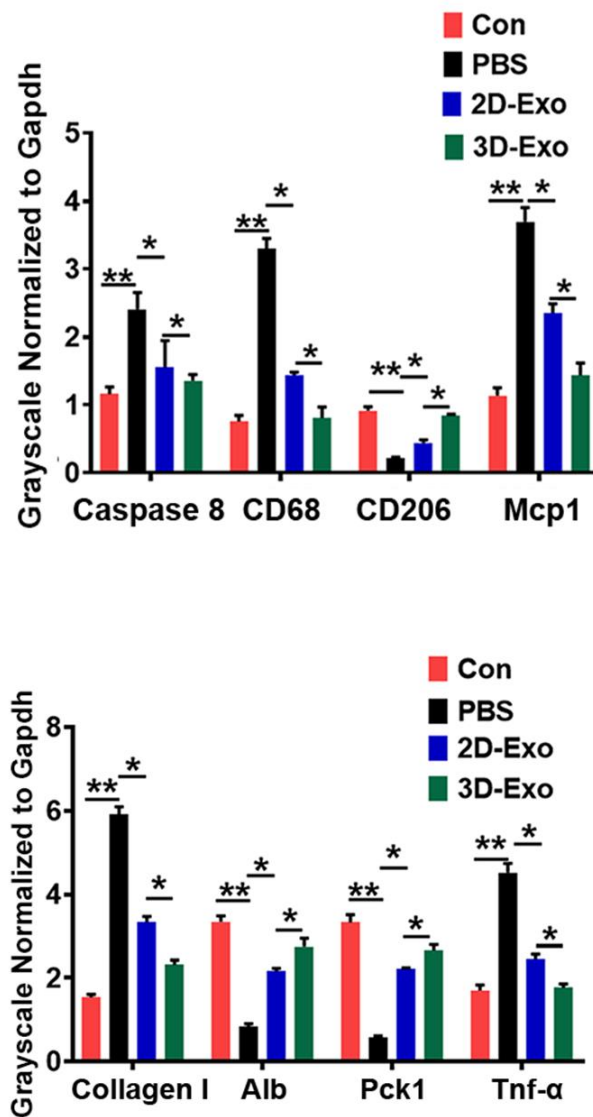


Figure S6. Apoptosis, inflammation and fibrosis could be weakened by hESC-exosomes in the livers of fibrosis mice.

According to Western blot analysis in Fig. 4f, corresponding densitometry for the protein levels of Collagen I, Alb, Pck1, Tnf- $\alpha$ , Caspase 8, CD68, CD206 and Mcp1

were quantitated in the liver tissues of the fibrosis mice with different treatments.

Gapdh was used as a loading control. n=3, Data represent the mean  $\pm$ SEM. \* $P < 0.05$ ,

\*\* $P < 0.01$ , and \*\*\* $P < 0.001$ .

**Figure. S7**

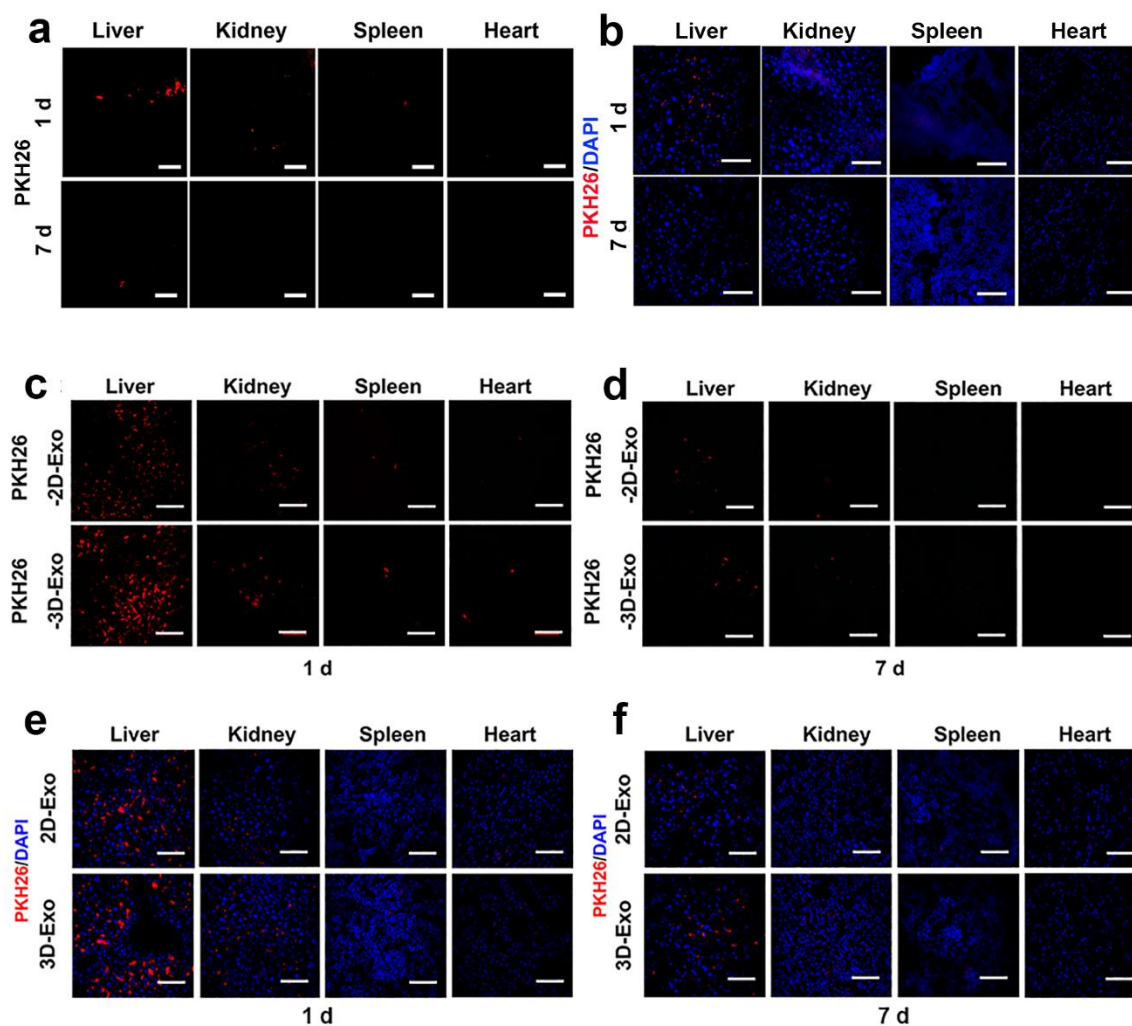


**Figure S7. In vivo tracking of PKH26 and PKH labeled-Exos in mice.**

(a) *In vivo* TPEF imaging of major organs (liver, kidney, spleen and heart) in PKH26-alone -treated mice on days 1 and 7. (b) *Ex vivo* CLSM imaging of major organs (liver, kidney, spleen and heart) dissected from sacrificed the mice on days 1 and 7. (c-d) The enrichment and metabolism of PKH26 labeled-exosomes in liver, kidney, spleen and heart were imaged using TPEF at 1d and 7d after caudal vein injection (Original magnification, 25 $\times$ , Scale bar, 40 $\mu$ m). (e-f) *Ex vivo* CLSM imaging of major organs

(liver, kidney, spleen and heart) dissected from sacrificed the mice on days 1 and 7.

(Original magnification, 20×, Scale bar, 40μm).

**Figure. S8**

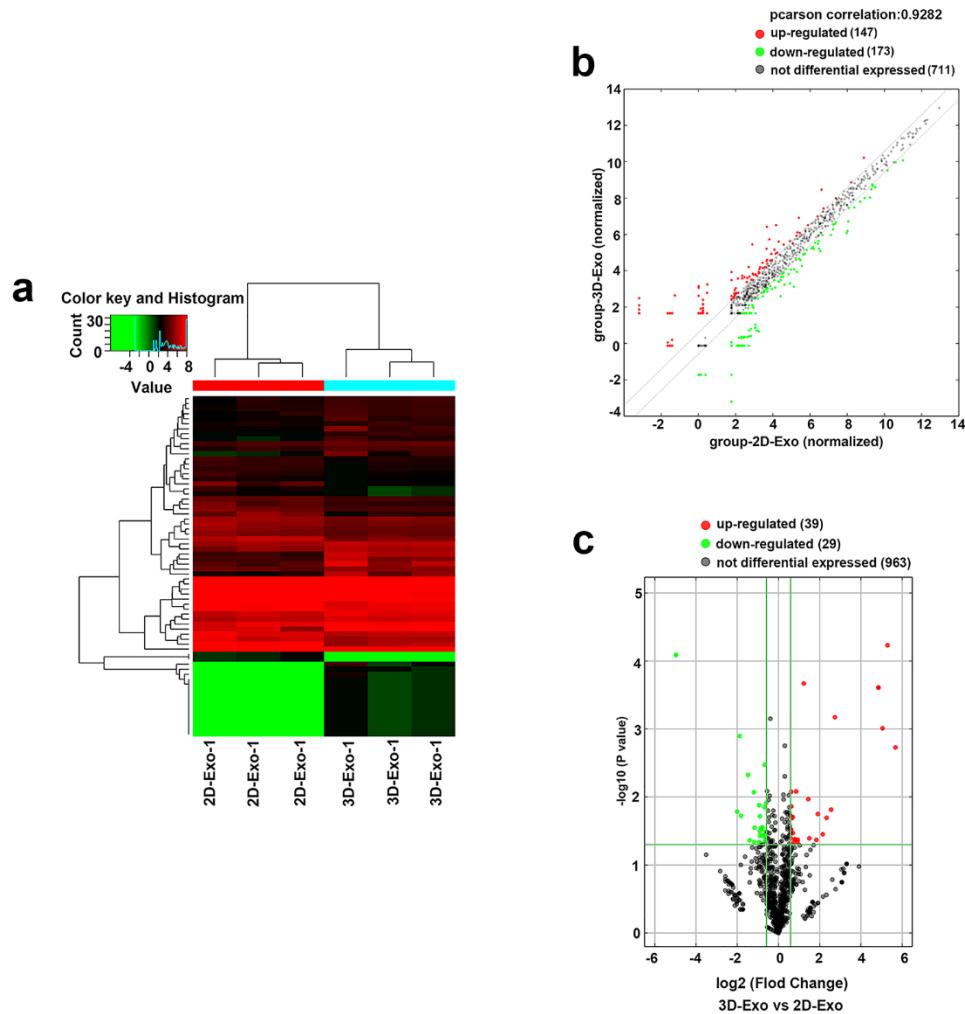


**Figure S8. Microarray analysis of miRNAs between 2D-Exo and 3D-Exo.**

(a) Microarray heat map representing distinct miRNA expression values in 3D-Exo compared with 2D-Exo controls (fold change $\geq$ 2,  $P < 0.05$ ). Red color scale: higher expression. Green color scale: lower expression.  $n = 3$  samples/group. Statistical significance was evaluated by using Student's t-test and corrected for multiple testing by using the Benjamini & Hochberg method. (b) Standardization of the above image showed differentially expressed genes between the two groups. (c) Difference analysis

between 2D-Exo and 3D-Exo groups of miRNA expression volcano map. Using  $\log_2$  Fold Change (FC)  $> 1$  and adjusted p-value  $< 0.01$  as the screening criteria, 39 up-regulated miRNAs and 29 down-regulated miRNAs were screened.

**Figure. S9**

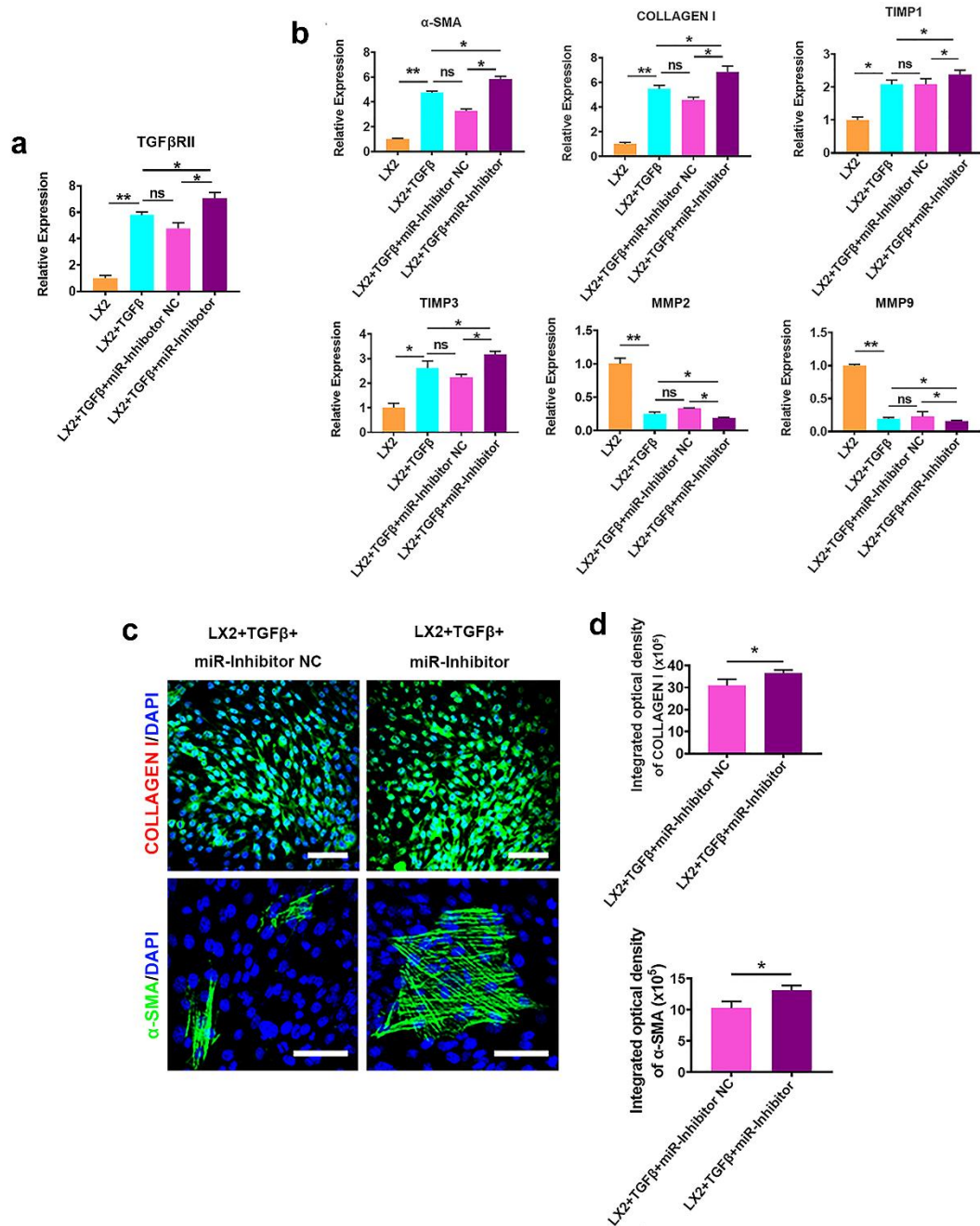


**Figure S9. The knockdown of miR-6766-3p by inhibitor upregulated profibrogenic markers of activated LX2 cells.**

(a) The expression level of TGFβRII genes determined by qPCR was increased in activated LX2 cells after coculture with miR-6766-3p inhibitor NC and miR-6766-3p inhibitor for 48 hours. (b) The knockdown of miR-6766-3p upregulated profibrogenic-

related genes ( $\alpha$ -SMA, COLLAGEN I, TIMP1, TIMP3), and downregulated MMP2 and MMP9 in activated LX2 cells after co-culture with miR-6766-3p inhibitor NC and miR-6766-3p inhibitor for 48 hours, as determined by qPCR. (c) The positive cell number of COLLAGEN I and  $\alpha$ -SMA was increased in activated LX2 cocultured with miR-6766-3p inhibitor for 48 hours. (d) Quantification of integrated optical density of COLLAGEN I and  $\alpha$ -SMA in (c) showed a significant increase in miR-6766-3p inhibitor group. Magnification, 20 $\times$ , 40 $\mu$ m; Green (COLLAGEN I;  $\alpha$ -SMA) and DAPI (blue) were shown. n=3, Data represent the mean  $\pm$  SEM. \* $P$  < 0.05, \*\* $P$  < 0.01, and \*\*\* $P$  < 0.001.

**Figure. S10**

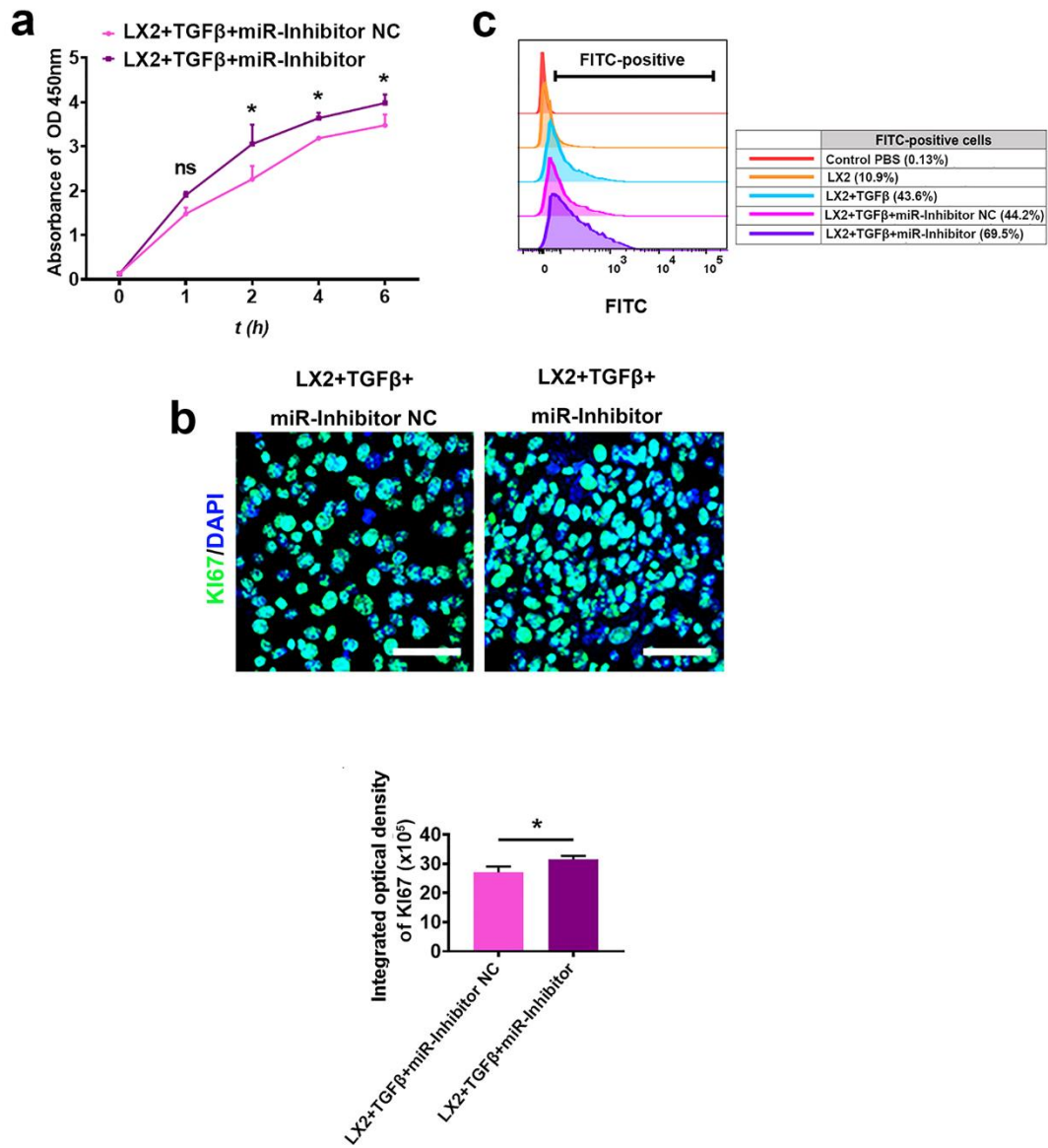


**Figure S10. The knockdown of miR-6766-3p by inhibitor enhanced proliferation of LX2 cells.**

(a) The inhibitory effect of miR-6766-3p on activated LX2 cell proliferation was reversed by the knockdown of miR-6766-3p with inhibitor, as measured using CCK8 assays at 2, 4 and 6 hours after exposure to miR-6766-3p inhibitor NC or miR-6766-3p inhibitor. (b) The expression of Ki67 was detected by the immunostaining in activated

LX2 cocultured with miR-6766-3p inhibitor NC and miR-6766-3p inhibitor for 48 hours. Quantification of integrated optical density of KI67 showed a significant increase by miR-6766-3p inhibitor. Magnification, 20 $\times$ , 40 $\mu$ m; Green (KI67) and blue (DAPI) were shown. (c) Flow cytometry results showed that the increase in calcium content after TGF $\beta$ -induced activation of LX2 could be further activated by miR-6766-3p inhibitor, indicating the enhancement of activated LX2 cells by the knockdown of miR-6766-3p. n=3, Data represent the mean  $\pm$  SEM. \*P < 0.05, \*\*P < 0.01, and \*\*\*P < 0.001.

**Figure. S11**

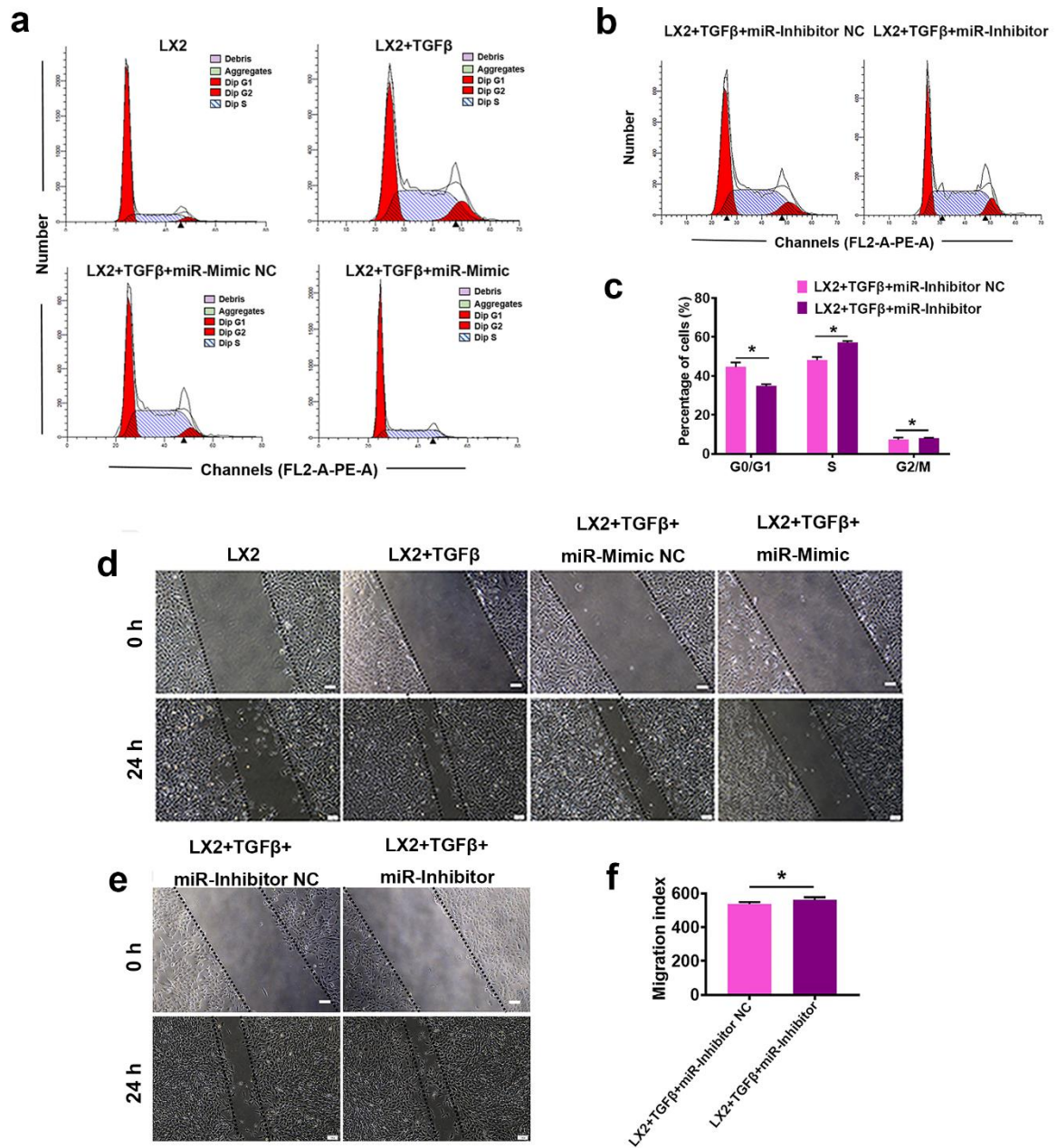


**Figure S11. miR-6766-3p modulated cell cycle and migration of LX2 cells.**

(a) Cell cycle analysis showed that the growth of activated LX2 cells exposed to 2D-Exo or 3D-Exo was significantly inhibited by showing lower percentage of S phase LX2 cells, when compared to the TGF $\beta$ -induced LX2 cells. (b-c) LX2 cell cycle distribution after growth in co-cultures with miR-6766-3p inhibitor NC and miR-6766-

3p inhibitor for 48 hours. The percentage of S phase LX2 cells significantly increased in miR-6766-3p inhibitor at 48 hours, indicating that the knockdown of miR-6766-3p promoted the growth of activated LX2 cells. (d) Wound recovery rates of activated LX2 cells was decreased by miR-6766-3p mimic, when compared to activated LX2 cells and the treatment group with miR-6766-3p mimic NC, as modeled by cell scratch assays (Original magnification, 4×, Scale bar, 100µm). (e-f) The decrease of wound recovery rates of active LX2 cells was inhibited by the knockdown of miR-6766-3p with the inhibitor, compared with the cells treated with miR-6766-3p inhibitor NC, as determined by cell scratch assays. n=3, Data represent the mean ± SEM. \*P < 0.05, \*\*P < 0.01, and \*\*\*P < 0.001.

Figure. S12

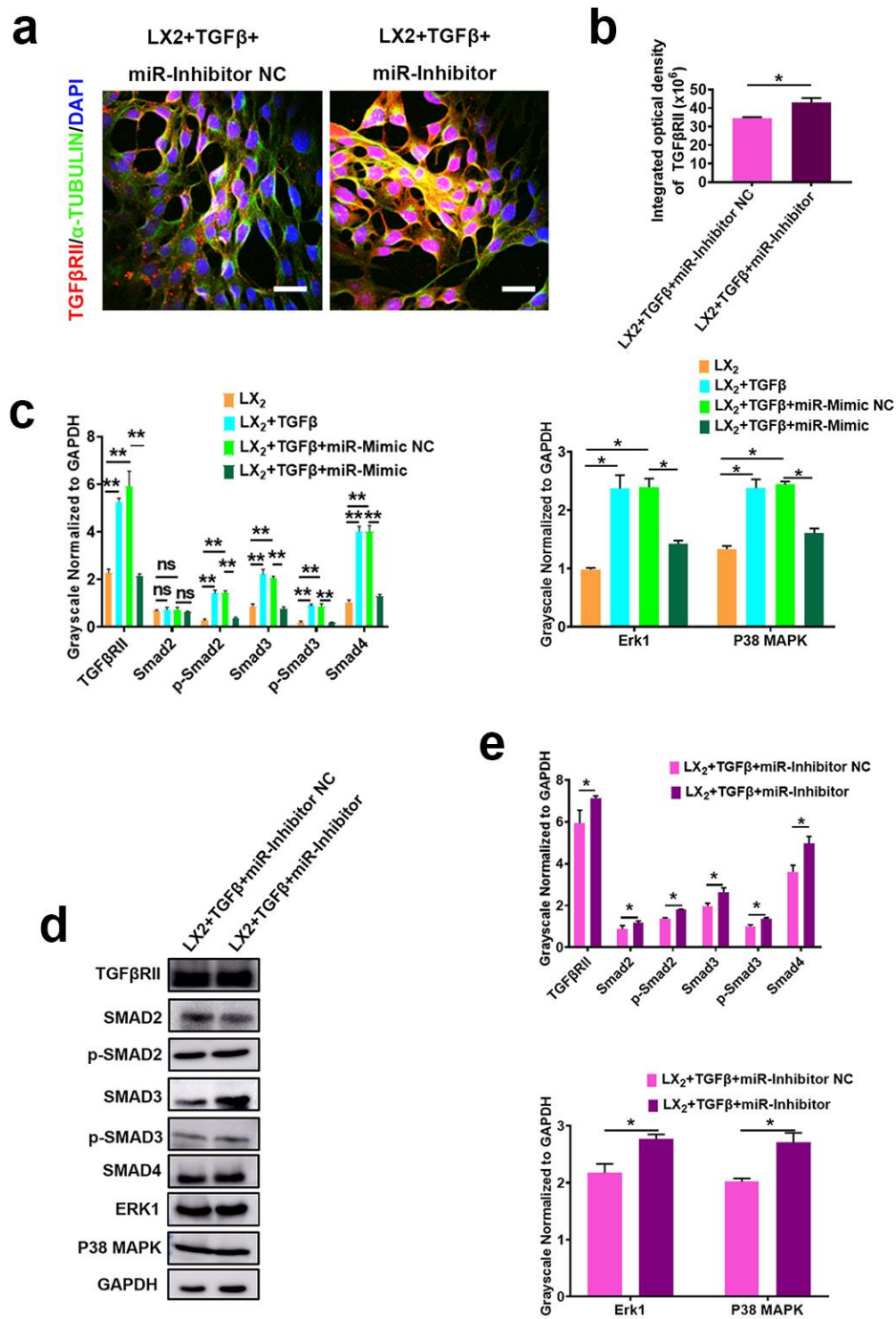


Figure S12. The knockdown of miR-6766-3p upregulated the expression of TGFβRII and activated the downstream Smads pathway.

(a) The percentage of positive cells for TGF $\beta$ RII determined by immunostaining was increased in activated LX2 co-cultured with miR-6766-3p inhibitor NC and miR-6766-3p inhibitor for 48 hours, indicating that the expression of TGF $\beta$ RII was upregulated by the knockdown of miR-6766-3p. (b) Quantification of integrated optical density of TGF $\beta$ RII in (a) showed significantly increases in the miR-6766-3p inhibitor group. Magnification, 20 $\times$ , 40  $\mu$ m; Green ( $\alpha$ -Tubulin), Red (TGF $\beta$ RII) and DAPI (blue) were shown. (c) According to Western blot analysis in Fig. 8c, quantification for the expression changes of TGF $\beta$ RII-mediated fibrosis pathway-associated proteins after miR-6766-3p overexpression in TGF $\beta$  treated LX2 cells. (d-e) Representative Western blot and corresponding densitometry analyses of markers, TGF $\beta$ RII, p-SMAD2, SMAD3, p-SMAD3, SMAD4 and non-SMADs proteins, ERK1 and P38 MAPK in activated LX2 co-cultured with miR-6766-3p inhibitor NC and miR-6766-3p inhibitor for 48 hours. miR-6766-3p inhibitor increased the expression of the ERK1 and P38 MAPK as well as the expression of SMADs. n=3, Data represent the mean  $\pm$ SEM. \* $P < 0.05$ , \*\* $P < 0.01$ , and \*\*\* $P < 0.001$ .

Figure S13

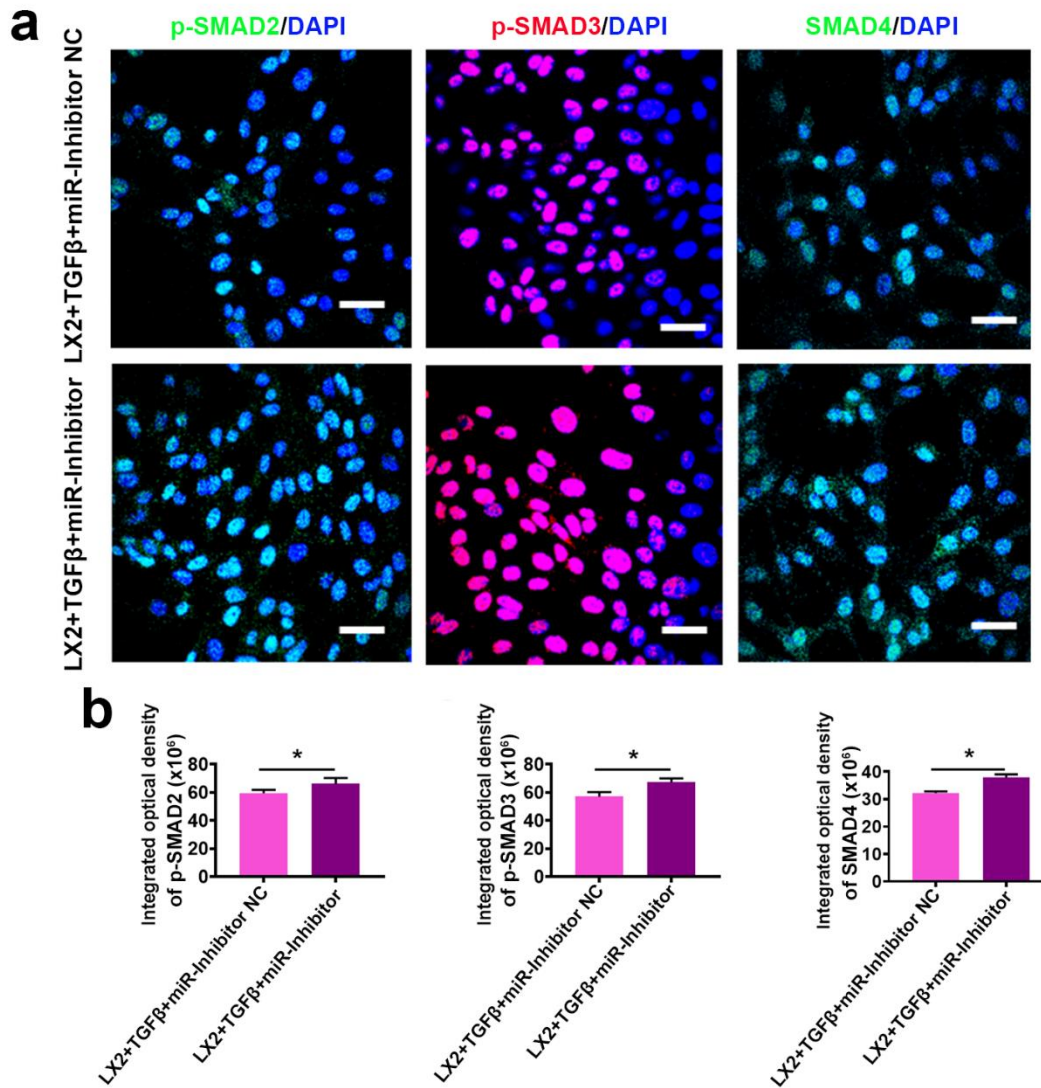
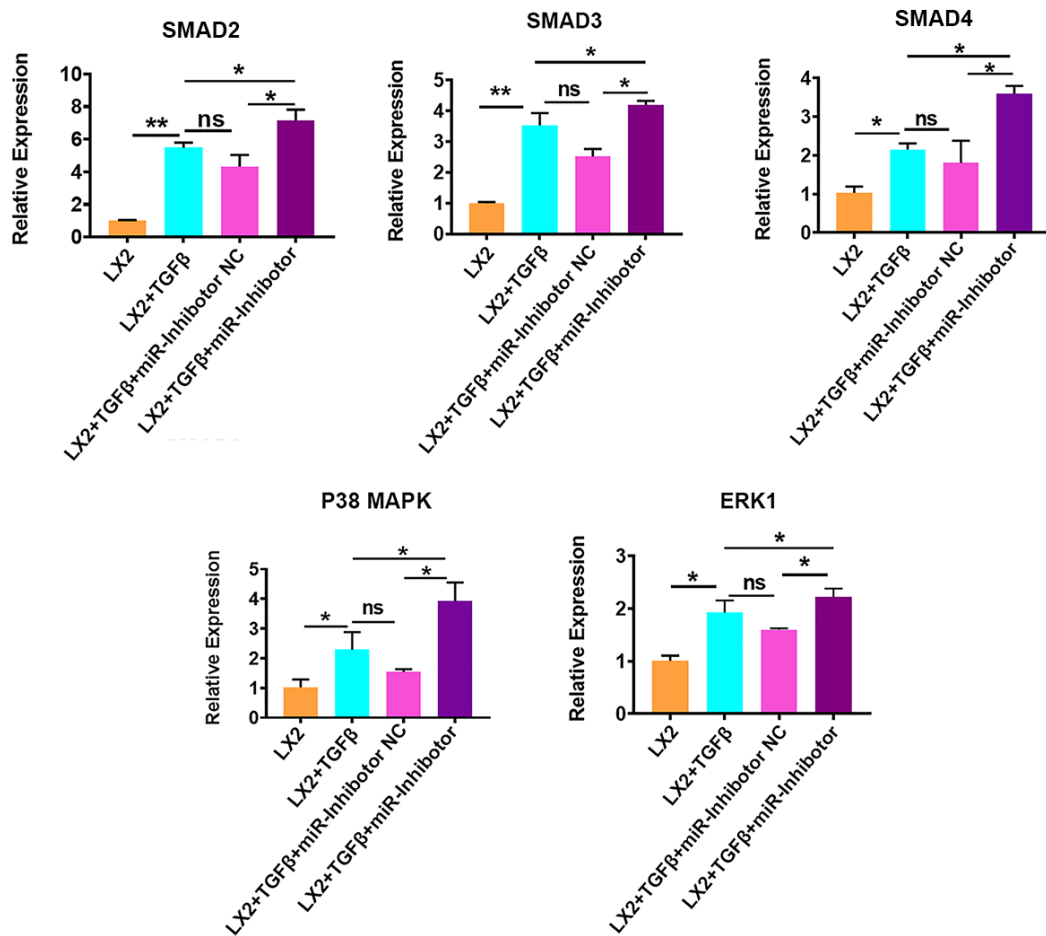


Figure S13. The knockdown of miR-6766-3p by the inhibitor activated the expression of the downstream Smads pathway.

(a) The percentage of positive nuclear staining for p-SMAD2, p-SMAD3 and SMAD4 measured by immunostaining was increased in activated LX2 cells co-cultured with miR-6766-3p inhibitor NC and miR-6766-3p inhibitor for 48 hours, indicating that the expression of SMADs were upregulated by the knockdown of miR-6766-3p with the inhibitor. (b) Quantification of integrated optical density in (a) showed that the cell

number of positive nuclear staining of p-SMAD2, p-SMAD3 and SMAD4 significantly was increased in activated LX2 cells treated with miR-6766-3p inhibitor. Magnification, 20×, 40μm; Green (p-SMAD2; SMAD4), Red (p-SMAD3) and DAPI (blue) were shown. n=3, Data represent the mean ±SEM. \* $P < 0.05$ , \*\* $P < 0.01$ , and \*\*\* $P < 0.001$ .

**Figure S14**



**Figure S14. The inhibition of miR-6766-3p upregulated the gene expression of SMADs pathway.**

The expression level of SMADs genes was increased in activated LX2 cells after co-culture with miR-6766-3p inhibitor for 48 hours when compared to those co-culture with miR-6766-3p inhibitor NC.  $n=3$ , Data represent the mean  $\pm$  SEM. \* $P < 0.05$ , \*\* $P < 0.01$ , and \*\*\* $P < 0.001$ .

**Figure. S15**

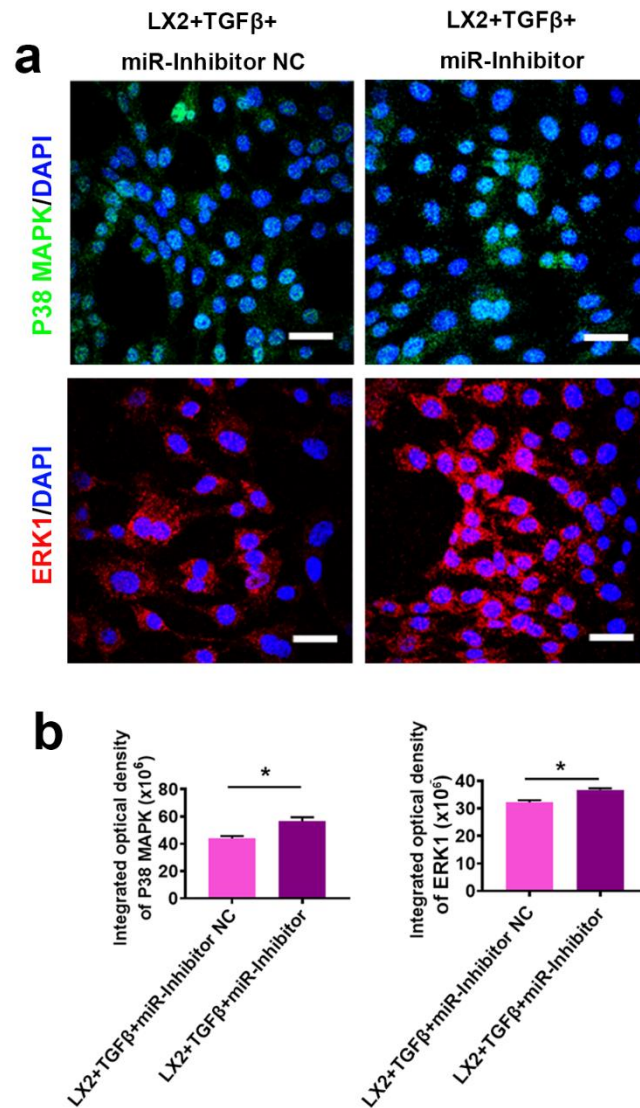


**Figure S15. The knockdown of miR-6766-3p activated the expression of the upstream modulators of SMADs pathway.**

(a-b) The number of positive cells for ERK1 and P38 MAPK, the upstream modulators of SMADs pathway was increased in activated LX2 cells co-cultured with miR-6766-3p inhibitor NC and miR-6766-3p inhibitor for 48 hours, as determined by immunostaining using CLSM images, indicating that miR-6766-3p inhibitor increased the expression of ERK1 and P38 MAPK, consequently leading to the expression of

SMADs. (Original magnification, 20 $\times$ . Scale bar, 40 $\mu$ m). n=3, Data represent the mean  $\pm$ SEM. \*P < 0.05, \*\*P < 0.01, and \*\*\*P < 0.001.

## Supporting Tables

**Table S1. Primers for mRNA qPCR**

Name	Sequences	Providers
hSOX2-qF	CGATGTACAACATGATGGAGACGGAGCT	Sangon
		Biotech
hSOX2-qR	ATTCACATGTGTGAGAGGGGCAGT	Sangon
		Biotech
hOCT4-qF	ATATGGCGGGACACCTGGCTT	Sangon
		Biotech
hOCT4-qR	CGTCAGTTTGAATGCATGGGAGAGC	Sangon
		Biotech
hNANOG-qF	ATATGAGTGTGGATCCAGCTTGTC	Sangon
		Biotech
hNANOG-qR	CGTCACACGTCTTCAGGTTGCATGTT	Sangon
		Biotech
hCOLLAGEN I-qF	ATGTCTAGGGTCTAGACATGTTCA	Sangon
		Biotech
hCOLLAGEN I-qR	CCTTGCCGTTGTCGCAGACG	Sangon
		Biotech
hRHOA-qF	GGACTCGGATTCGTTGCCT	Sangon
		Biotech

h <i>RHOA</i> -qR	CCATCACCAACAATCACCAGTT	Sangon
		Biotech
h <i>CYCLIN D</i> -qF	CATCTACACCGACAACCTCCATC	Sangon
		Biotech
h <i>CYCLIN D</i> -qR	TCTGGCATT TTTGGAGAGGAAG	Sangon
		Biotech
h <i>RAC1</i> -qF	CCCAATACTCCTATCATCCTCG	Sangon
		Biotech
h <i>RAC1</i> -qR	CAGCAGGCATT TTTCTCTTCC	Sangon
		Biotech
h <i>CDC42</i> -qF	GCCCGTGACCTGAAGGCTGTCA	Sangon
		Biotech
h <i>CDC42</i> -qR	TGCTTTTAGTATGATGCCGACACCA	Sangon
		Biotech
h $\alpha$ - <i>SMA</i> -qF	ACTGAGCGTGGCTATTCCTCCGTT	Sangon
		Biotech
h $\alpha$ - <i>SMA</i> -qR	GCAGTGGCCATCTCATT T TCA	Sangon
		Biotech
h <i>P27</i> -qF	TGCAACCGACGATTCTTCTACTCAA	Sangon
		Biotech

hP27-qR	CAAGCAGTGATGTATCTGATAAACAAGGA	Sangon
		Biotech
hTIMP1-qF	TTGTGGGACCTGTGGAAGTA	Sangon
		Biotech
hTIMP1-qR	CTGTTGTTGCTGTGGCTGAT	Sangon
		Biotech
hMMP2-qF	GATACCCCTTTGACGGTAAGGA	Sangon
		Biotech
hMMP2-qR	CCTTCTCCCAAGGTCCATAGC	Sangon
		Biotech
hMMP9-qF	GGGACGCAGACATCGTCATC	Sangon
		Biotech
hMMP9-qR	TCGTCATCGTCGAAATGGGC	Sangon
		Biotech
hTIMP3-qF	CTGACAGGTCGCGTCTATGA	Sangon
		Biotech
hTIMP3-qR	GGCGTAGTGTTTGGACTGGT	Sangon
		Biotech
hP38 MAPK-qF	AAGACTCGTTGGAACCCAG	Sangon
		Biotech

<i>hP38 MAPK</i> -qR	TCCAGTAGGTCGACAGCCAG	Sangon
		Biotech
<i>hSMAD4</i> -qF	CCAATCATCCTGCTCCTGAGT	Sangon
		Biotech
<i>hSAM4</i> -qR	CCAGAAGGGTCCACGTATCC	Sangon
		Biotech
<i>hTGFβRII</i> -qF	GTGAGAAGCCGCAGGAAGTC	Sangon
		Biotech
<i>hTGFβRII</i> -qR	CCGTGGTAGGTGAACTTGGG	Sangon
		Biotech
<i>hSMAD3</i> -qF	CATCGAGCCCCAGAGCAATA	Sangon
		Biotech
<i>hSMAD3</i> -qR	GTGGTTCATCTGGTGGTCACT	Sangon
		Biotech
<i>hERK1</i> -qF	CCTGCGACCTTAAGATTTGTGATT	Sangon
		Biotech
<i>hERK1</i> -qR	CAGGGAAGATGGGCCGGTTAGAGA	Sangon
		Biotech
<i>hSMAD2</i> -qF	CCGACACACCGAGATCCTAAC	Sangon
		Biotech

hSMAD2-qR	AGGAGGTGGCGTTTCTGGAAT	Sangon
		Biotech
hGAPDH-qF	GAAGATGGTGATGGGATTTC	Sangon
		Biotech
hGAPDH-qR	GAAGGTGAAGGTCGGAGTC	Sangon
		Biotech
mCollagen I-qF	TGACTGGAAGAGCGGAGAGT	Sangon
		Biotech
mCollagen I-qR	GACGGCTGAGTAGGGAACAC	Sangon
		Biotech
m $\alpha$ -SMA-qF	GAGGCACCACTGAACCCTAA	Sangon
		Biotech
m $\alpha$ -SMA-qR	CATCTCCAGAGTCCAGCACA	Sangon
		Biotech
mIl6-qF	GAGGATACTCACTCCCAACAGACC	Sangon
		Biotech
mIl6-qR	AAGTGCATCATCGTTGTTTCATACA	Sangon
		Biotech
mTgfb-qF	CAACAATTCCTGGCGTTACCTTGG	Sangon
		Biotech

<i>mTgfb</i> -qR	GAAAGCCCTGTATTCCGTCTCCTT	Sangon
		Biotech
<i>mIfny</i> -qF	GGCCATCAGCAACAACATAAGCGT	Sangon
		Biotech
<i>mIfny</i> -qR	TGGGTTGTTGACCTCAAACCTTGGC	Sangon
		Biotech
<i>mCaspase 8</i> -qF	ATCTGGCTCGGGGTTACTG	Sangon
		Biotech
<i>mCaspase 8</i> -qR	CTGCGTGGTGGTCATTCTC	Sangon
		Biotech
<i>mHgf</i> -qF	GAACTGCAAGCATGATGTGG	Sangon
		Biotech
<i>mHgf</i> -qR	GATGCTGGAAATAGGGCAGAA	Sangon
		Biotech
<i>mHss</i> -qF	GCGCAAGGCATAGAGACGA	Sangon
		Biotech
<i>mHss</i> -qR	GTCCGCATCCACGACTTGAA	Sangon
		Biotech
<i>mGapdh</i> -qF	TTGTCTCCTGCGACTTCAAC	Sangon
		Biotech

m*Gapdh*-qR

GTCATACCAGGAAATGAGCTTG

Sangon

Biotech

---

**Table S2. Primers for miRNA qPCR**

Name	Sequences	Providers
<i>hsa-miR-4728-5p-qF</i>	GTCGTATCCAGTGCAGGGTCCGAGGT ATTCGCACTGGATACGACTGCTTG	Sangon Biotech
<i>hsa-miR-6734-5p-qF</i>	GTCGTATCCAGTGCAGGGTCCGAGGT ATTCGCACTGGATACGACTCTCCA	Sangon Biotech
<i>hsa-miR-3652-qF</i>	GTCGTATCCAGTGCAGGGTCCGAGGT ATTCGCACTGGATACGACTCCTCA	Sangon Biotech
<i>hsa-miR-6793-5p-qF</i>	GTCGTATCCAGTGCAGGGTCCGAGGT ATTCGCACTGGATACGACTCACCC	Sangon Biotech
<i>hsa-miR-6766-3p-qF</i>	GTCGTATCCAGTGCAGGGTCCGAGGT ATTCGCACTGGATACGACTGAGGG	Sangon Biotech
<i>hsa-miR-6785-5p-qF</i>	GTCGTATCCAGTGCAGGGTCCGAGGT ATTCGCACTGGATACGACCACCAT	Sangon Biotech
<i>hsa-miR-500a-5p-qF</i>	GTCGTATCCAGTGCAGGGTCCGAGGT ATTCGCACTGGATACGACTCTCAC	Sangon Biotech
<i>hsa-miR-6511b-5p-qF</i>	GTCGTATCCAGTGCAGGGTCCGAGGT ATTCGCACTGGATACGACTGTCAG	Sangon Biotech
<i>hsa-miR-4690-5p-qF</i>	GTCGTATCCAGTGCAGGGTCCGAGGT ATTCGCACTGGATACGACTTCAGC	Sangon Biotech

<i>hsa-miR-5194-qF</i>	GTCGTATCCAGTGCAGGGTCCGAGGT	Sangon
	ATTCGCACTGGATACGACCCATCC	Biotech
<i>hsa-miR-4259-qF</i>	GTCGTATCCAGTGCAGGGTCCGAGGT	Sangon
	ATTCGCACTGGATACGACTCCTGA	Biotech
<i>U6-qF</i>	AAAATATGGAACGCTTCACGAATTTG	Sangon
		Biotech
<i>hsa-miR-qR</i>	AGTGCAGGGTCCGAGGTATT	Sangon
		Biotech

---

**Table S3. Primers for miRNA PCR**

<b>Name</b>	<b>Sequences</b>	<b>Providers</b>
<i>hsa-miR-4728-5p-F</i>	TGGGAGGGGAGAGGCAG	Sangon Biotech
<i>hsa-miR-6734-5p-F</i>	GCGTTGAGGGGAGAATGAGG	Sangon Biotech
<i>hsa-miR-3652-F</i>	CGCGCGGCTGGAGGTG	Sangon Biotech
<i>hsa-miR-6793-5p-F</i>	GCGTGTGGGTTCTGGGTTG	Sangon Biotech
<i>hsa-miR-6766-3p-F</i>	GCGTGATTGTCTTCCCCCA	Sangon Biotech
<i>hsa-miR-6785-5p-F</i>	TGGGAGGGCGTGGATG	Sangon Biotech
<i>hsa-miR-500a-5p-F</i>	CGCGTAATCCTTGCTACCTGG	Sangon Biotech
<i>hsa-miR-6511b-5p-F</i>	CTGCAGGCAGAAGTGGGG	Sangon Biotech
<i>hsa-miR-4690-5p-F</i>	GGAGCAGGCGAGGCTGG	Sangon Biotech
<i>hsa-miR-5194-F</i>	GCGTGAGGGGTTTGAATG	Sangon Biotech
<i>hsa-miR-4259-F</i>	CGCAGTTGGGTCTAGGGG	Sangon Biotech
<i>U6-F</i>	CTCGCTTCGGCAGCACATATACT	Sangon Biotech
<i>hsa-miR-R</i>	ACGCTTCACGAATTTGCGTGTC	Sangon Biotech

**Table S4. Antibodies used in this study**

<b>Name</b>	<b>Species reactivity</b>	<b>Applications</b>	<b>Providers</b>	<b>Cat. No.</b>
anti-CD9	Human, Mouse, Rat	WB (1:500)	Bioss	bs-2489R
anti-CD63	Human	WB (1:500)	Bioss	bs-1523R
anti- $\alpha$ -SMA	Human, Mouse, Rat	WB (1:1000); IF (1:200)	CST	48938S
anti-collagen I	Human, Mouse, Rat, Rabbit	WB (1:500); IF (1:100)	Bioss	bs-10423R
anti-CDC42	Mouse, Rat, Human	WB (1:10000); IF (1:500)	Abcam	ab187643
anti-TGF $\beta$ 1	Mouse, Rat, Human	WB (1:500); IF (1:100)	Bioss	bs-0086R
anti-RhoA	Mouse, Rat, Human	WB (1:5000); IF (1:150)	Abcam	ab187027
anti-GAPDH	Mouse, Rat, Human	WB (1:1000)	CST	5174s
anti-F4/80	Mouse	IHC (1:400)	CST	30325T
anti-iNOS	Mouse	IHC (1:400)	CST	13120S

anti-TNF $\alpha$	Mouse	IHC (1:400)	CST	11948T
anti-PCNA	Mouse, Rat, Human	IHC (1:25)	Abce	AW5198
			pta	
anti-ALB	Human, Mouse	WB (1:1000)	Abce	AP6540
			pta	B
anti-PCK1	Mouse, Rat, Human	WB (1:1000)	Abca	ab28455
			m	
anti-	Human, Mouse	WB (1:2000)	Bioss	bsm-
caspase8				33190M
anti-CD68	Mouse, Rat, Human	WB (1:1000)	Abca	ab955
			m	
anti-CD206	Mouse, Rat, Human	WB (1:1000)	Abca	ab64693
			m	
anti-MCP1	Mouse, Rat, Human	WB (1:1000)	Novu	NBP1-
			s	07035SS
anti-Ki67	Human	IF (1:400)	CST	9449
anti-	Mouse, Rat, Human	WB (1:500)	Bioss	bs-
TGF $\beta$ RII				0117R
anti- $\alpha$ -	Mouse, Rat, Human	IF (1:1000)	CST	3873s
Tubulin				

anti-p-SMAD2	Mouse, Rat, Human	WB (1:1000)	CST	18338T
anti-p-SMAD3	Mouse, Human	WB (1:2000)	Abcam	Ab52903
anti-SMAD4	Mouse, Rat, Human	WB (1:1000); IF (1:800)	CST	46535T
anti-SMAD2	Mouse, Rat, Human	WB (1:1000); IF (1:100)	CST	5339T
anti-SMAD3	Mouse, Rat, Human	WB (1:1000); IF (1:100)	CST	9523T
anti-ERK1	Mouse, Human	WB (1:1000); IF (1:400)	Abcam	Ab32537
anti-P38 MAPK	Mouse, Rat, Human	WB (1:1000); IF (1:200)	CST	8690T
anti-SOX2	Mouse, Human	IF (1:400)	CST	4900
anti-OCT4	Human	IF (1:200)	CST	2750
PE Anti-OCT4	Human	FlowCytometry (5ul/Test)	STEMCELL	60093PE

PE Anti-SSEA-4	Human	FlowCytometry (5ul/Test)	STE M CEL L	60062PE
PE Anti-TRA-1-81	Human	FlowCytometry (5ul/Test)	STE M CEL L	60065PE
PE-Cy™5 Mouse IgG1 κ Isotype Control	Human	FlowCytometry (20ul/Test)	BD	555750
Anti-mouse IgG (H+L) F(ab')2 Fragment (Alexa Fluor 594 Conjugate)	mouse	IF (1:1000)	CST	8890S
Anti-mouse IgG	mouse	IF (1:1000)	CST	4408s

(H+L)F(ab')

2 Fragment

(Alexa Fluor

488

Conjugate)

Anti-rabbit rabbit

IF (1:1000)

CST 8889s

IgG (H+L)

F(ab')<sub>2</sub>

Fragment

(Alexa Fluor

594

Conjugate)

Anti-rabbit rabbit

IF (1:1000)

CST 4412s

IgG

(H+L)F(ab')

2 Fragment

(Alexa Fluor

488

Conjugate)

Anti-rabbit rabbit

WB (1:1000)

CST 7074s

IgG HRP-

linked

Antibody

Anti-mouse mouse WB (1:1000) CST 7076S

IgG HRP-

linked

Antibody

---